ACADEMIA ROMÂNĂ
Revue Roumaine de Chimie
https://www.icf.ro/rrch/

Rev. Roum. Chim.,
2023, *68*(9), 435–446
DOI: 10.33224/rrch.2023.68.9.04

CORROSION INHIBITION EFFICIENCY OF QUINOXALINES BASED ON ELECTRONIC STRUCTURE AND QUANTUM COMPUTATIONAL ANALYSIS

Dyari Mustafa MAMAND and Hiwa Mohammad QADR*

University of Raparin, College of Science, Department of Physics, Sulaymaniyah, Iraq

Received November 16, 2022

Based on the quantum chemical parameters obtained from density functional theory (DFT) with 6-311++ G (d, p) basis set at B3LYP level, a theoretical study of the corrosion inhibition effectiveness of 1-[4-acetyl-2-(4-chlorophenyl) quinoxalin-1(4H)-yl] acetone (A), 2-(4-(2-ethoxy-2-oxoethyl)-2-p-tolylquinoxalin-1(4H)-yl) acetate (B) and 2-(4-methylphenyl)-1,4-dihydroquinoxaline (C) were evaluated. A number of quantum chemical parameters were determined to assess the array of molecules selected, including lowest unoccupied molecular orbital energy, highest occupied molecular orbital energy, hardness, ionization potential, the electronegativity, dipole moment, the fraction of electrons transferred to the metal surface, total energy and softness. Experiments were found to be in agreement with theoretical data.

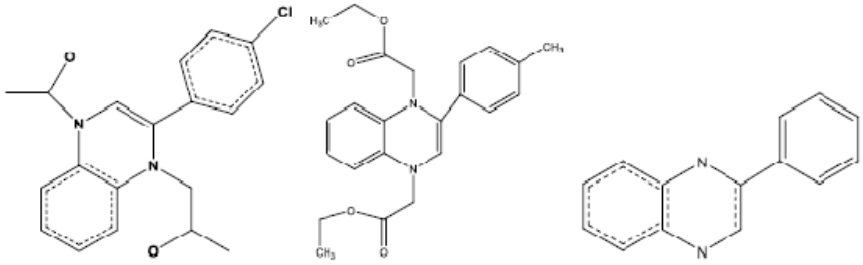

INTRODUCTION

Metal corrosion resistance is a major problem in industry and science. Inhibitors are one of the most practical ways to prevent corrosion, especially in acidic environments.[1] Inhibitors can adhere to metallic surfaces to provide a protective barrier versus corrosive chemicals that come into contact with it.[2] The contact between inhibitor and metal surface determine how successful an inhibitor is in providing corrosion protection.[3] The effect of adsorption inhibitors on the corrosion of the metal reaction surface can be attributed to the difference in the activation barriers of the cathodic and anodic interactions of the corrosive environment, or it can be related to the blocking effect of the adsorption inhibition on the surface of the metal.[4] Excellent corrosion inhibitors can be considered to be such organic compounds which not only offer electrons to unoccupied d orbitals of the metal surface to form coordinate covalent bond, but also can accept the free electrons from the surface of the metal as well, by using their antibonding orbital to form feedback bonds in turn.[5–7] The physicochemical qualities of the inhibitor group such as p-orbital character, electronic density at the donor atom and functional group are exhibited to be significant in adsorption

* Corresponding author: hiwa.physics@uor.edu.krd

on metal surfaces, according to the researchers.[3,8,9] The efficiency of inhibition is also affected by the molecular electronic structure which includes the number of adsorption active centers such as O, S, and N atoms, the projected area of the inhibitor on the metallic surface, the mode of adsorption, the molecular size and the formation of metallic complexes.[10] The physicochemical properties of the inhibitor molecule, the nature and conditions of the metal surface and the type of corrosion media all influence the selection of a suitable inhibitor.[11] The majority of inhibitors were chosen based on an empirical understanding of their macroscopic physicochemical features. The efficiency of an inhibitor molecule has recently been linked to both spatial and electrical structures.[12,13] Quantum chemical approaches are an excellent tool for studying these characteristics since they can reveal information about the inhibitor-surface interaction.[14–16] In DFT, chemical properties of chemical compounds are measured, which allows us to compare molecules at the level of softness and hardness, which were first proposed by Pearson.[17] The inhibitors were chosen because they contain heteroatoms and π – electrons and such as N and O which leads to increased adsorption of the inhibitor compounds on the surface of the steel. The second compound is B which contains nitrogen as shown Fig. 1 which can give effective inhibition in acidic environments. The choice of the (C) compound was based on the fact that it comprises numerous – electrons and two N atoms, resulting in more inhibitor adsorption than compounds with only one N atom. Figure 1 shows chemical structures of investigated molecules. This paper investigates the electronic structure and level of corrosion rate for each of these molecules.

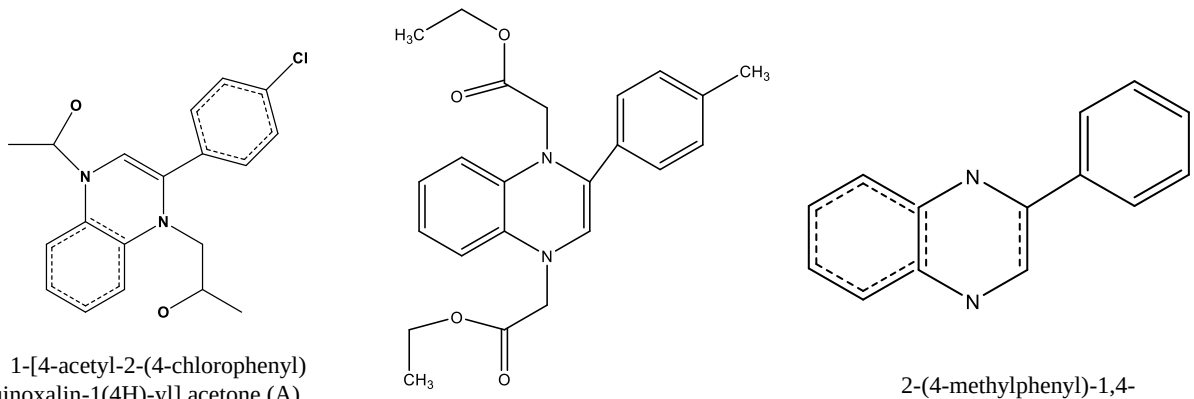

1-[4-acetyl-2-(4-chlorophenyl) quinoxalin-1(4H)-yl] acetone (A)

ethyl 2-(4-(2-ethoxy-2-oxoethyl)-2-p-tolylquinoxalin-1(4H)-yl) acetate (B)

2-(4-methylphenyl)-1,4-dihydroquinoxaline (C)

Fig. 1 – Chemical structures of inhibitors.

QUANTUM COMPUTATIONAL PARAMETERS

The goal of quantum chemical research is to interpret and characterize the molecular functionalities of these heterocyclic molecules. Theoretical computations were done to corroborate experimental results and give a molecular-level understanding comprehension of the experimentally which had been obtained behavior.[18–20] DFT has shown substantial promise among quantum chemical approaches for evaluating corrosion inhibitors, and it seems to be enough for pointing out the alterations in the electronic structure essential for inhibitory activity. In recent years, a hybrid version of DFT/HF methodologies like B3LYP has been effectively used to model systems including transition metal atoms.[21,22] DFT approach was used to perform computational chemistry procedures at the level of hybrid B3LYP functional theory using the 6-311++ G (d, p) basis which was developed by Gaussian 09 software series.[23,24] The analysis method was used to ensure that the molecules under study achieved the required base state. The ground state optimized geometries are found concerning the global minimum because all frequencies are positive. Since electrochemical corrosion usually happens in the aqueous phase, the effect of the solvent must be included in the computations. To calculate the effect of the solvent in the calculations, the continuous polarization method (PCM) was used. For a deeper understanding of the experimental results from the aqueous and gas phases, the self-consistent

reaction field method was combined with the polarized continuous Tommy model (PCM). In the DFT of Parr, Pearson and Yang, global electronic indexes are important essential for analyzing the sensitivity of molecules in their ground state.[14,25,26] As global or local reactivity characteristics, several parameters can be employed. Within the DFT, global hardness (η) is defined as the derivative of the E of regard to N at $\nu(r)$ characteristic, which assesses an atom's resistance to a charge transfer[27]

$$\eta = -\left(\frac{\partial^2 E}{\partial N^2}\right)_{v(r)} \quad (1)$$

Electronegativity is a measure of a group of atoms' abilities to attract electrons to itself when chemically bonded with another atom, and it may be denoted using the following expression in DFT[28]

$$\chi = -\left(\frac{\partial E}{\partial N}\right)_{v(r)} \quad (2)$$

where $\nu(r)$ is the nuclei's external potential, E is the electronic energy in electron volts and N is the number of electrons.[29] The following equations can calculate the electronegativity χ and hardness η:

$$\chi = \frac{I + A}{2} \quad (3)$$

$$\eta = \frac{I - A}{2} \quad (4)$$

Ionization potential and electron affinity are represented by I and A, respectively. The electron affinity (A) and ionization potential (I) of the inhibitors are estimated using the following formulae based on the total electronic energy values

$$I = E_{(N-1)} - E_N \quad (5)$$

$$A = E_N - E_{N+1} \quad (6)$$

The ground state energies of the system containing (N+1), (N–1), and (N) electrons are (N+1), (N–1), and (N), respectively. Electrons move from the lower electronegativity molecule to the greater electronegativity metal during the interaction of the inhibitor molecule with bulk metal until the chemical potential is equalized.[30] Equation 7 was used to calculate the proportion of transferred electrons, N

$$\Delta N = \frac{\chi_m - \chi_i}{2(\eta_m + \eta_i)} \quad (7)$$

where i and m denote the inhibitor molecule and metal atom individually and also denote the inhibitor molecule and the absolute electronegativity of iron sequentially. Furthermore, m and i denote the absolute hardness of iron and the inhibitor molecule, respectively. Using assumptions for a metallic bulk I = A, the theoretical values of m were 7 eV/mol and 0 eV/mol for bulk iron, respectively.

RESULT AND DISCUSSION

Quantum computational analysis

The optimized molecular structures of the studied quinoxalines derivatives are given in Fig. 2. Quantum chemical calculations are an essential tool for establishing a good association between molecular structure and corrosion prevention efficacy[31,32]. In contrast to Fukui's hypothesis, electron transitions are caused by interactions between reacting species HOMO and LUMO.

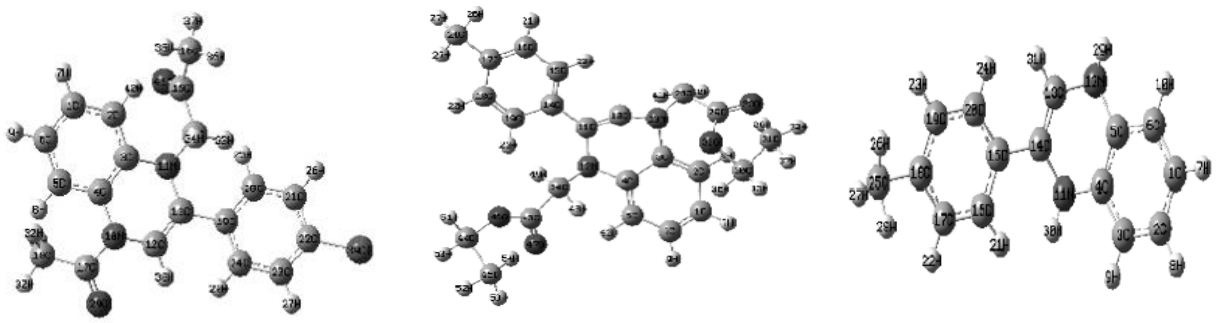

A B C

Fig. 2 – Optimized structures at 6-311++G(d, p) basis set.

Table 1

Theoretical calculations of molecular descriptors for neutral and cationic forms of compounds A, B, C, and D in gas and aqueous phases

Molecular descriptors	Gas phase		Aqueous phase	
	Non-protonated	Protonated	Non-protonated	Protonated
		Inhibitor A		
HOMO (eV)	–4.97424	–9.22902	–4.91139	-6.14488
LUMO (eV)	-1.0256	-5.08091	-1.17063	-2.09718
Dipole moment (Debye)	5.6730	8.9526	7.8436	11.9293
Total energy T.E (eV)	-1446.666	-1446.452	-1446.487	-1446.553
Ionization energy (eV)	4.974	9.229	4.911	6.144
Electron Affinity (eV)	1.025	5.080	1.170	2.097
Energy gap (eV)	3.948	4.148	3.740	4.047
Hardness (eV)	1.974	2.074	1.870	2.023
Softness (eV)	0.506	0.482	0.534	0.494
Electronegativity (eV)	2.999	7.154	3.041	4.121
Chemical potential (eV)	-2.999	-7.154	-3.041	-4.121
Electrophilicity (eV)	2.279	12.341	2.472	4.195
Nucleophilicity $(eV)^{-1}$	0.438	0.081	0.404	0.238
Back-donation (eV)	-0.493	-0.518	-0.467	-0.505
Electron transfer	1.013	-0.037	1.058	0.711
Initial molecule $\Delta\psi$	-2.026	-0.002	-2.094	-1.023
		Inhibitor B		
HOMO (eV)	-0.18482	-6.90162738	-3.93912226	-0.21837
LUMO (eV)	-0.04114	-3.09937846	-0.89443872	-0.17387
Dipole moment (Debye)	9.8440	13.6431	11.6968	13.3625
Total energy T.E (eV)	-1591.799	-1592.287	-1592.541	-1532.232
Ionization energy (eV)	5.029	6.901	3.939	5.942
Electron Affinity (eV)	1.119	3.099	0.894	4.731
Energy gap (eV)	3.909	3.802	3.044	1.210
Hardness (eV)	1.954	1.901	1.522	0.605
Softness (eV)	0.511	0.526	0.656	1.651
Electronegativity (eV)	3.074	5.000	2.416	5.336
Chemical potential (eV)	-3.074	-5.000	-2.416	-5.336
Electrophilicity (eV)	2.417	6.576	1.918	23.519
Nucleophilicity $(eV)^{-1}$	0.413	0.152	0.521	0.042
Back-donation (eV)	-0.488	-0.475	-0.380	-0.151
Electron transfer	1.004	0.525	1.505	1.373
Initial molecule $\Delta\psi$	-1.970	-0.525	-3.449	-1.142
		Inhibitor C		
HOMO (eV)	-7.61511029	-7.685	-4.9736	-8.9709
LUMO (eV)	-4.923630716	-3.2363	-0.6181	-4.0939
Dipole moment (Debye)	5.2201	7.6086	6.2322	5.0243
Total energy T.E (eV)	-685.460	-685.2504	-685.486	-685.613
Ionization energy (eV)	7.615	7.685	4.973	8.970
Electron Affinity (eV)	3.236	3.009	0.618	4.093
Energy gap (eV)	4.378	4.675	4.355	4.876
Hardness (eV)	2.189	2.337	2.177	2.438
Softness (eV)	0.456	0.427	0.459	0.410
Electronegativity (eV)	5.425	5.347	2.795	6.532
Chemical potential (eV)	-5.425	-5.347	-2.795	-6.532
Electrophilicity (eV)	6.722	6.116	1.794	8.749
Nucleophilicity $(eV)^{-1}$	0.148	0.163	0.557	0.114
Back-donation (eV)	-0.547	-0.584	-0.544	-0.609
Electron transfer	0.359	0.353	0.965	0.095
Initial molecule $\Delta\psi$	-0.282	-0.292	-2.029	-0.022

Gas phase	Aqueous phase
A: HOMO 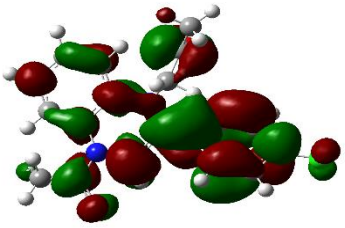	**A**: HOMO 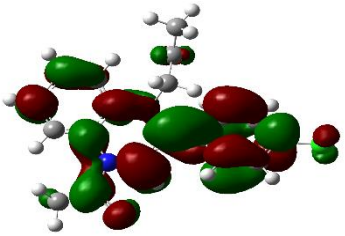
A: LUMO 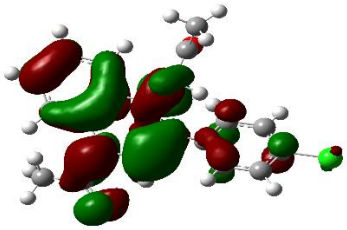	**A**: LUMO 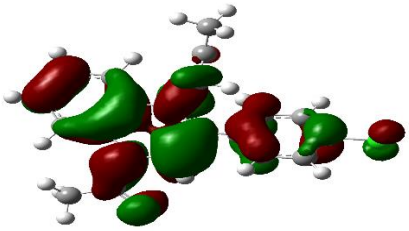
B: HOMO 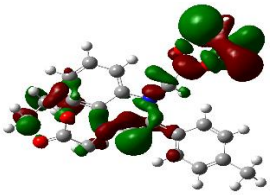	**B**: HOMO 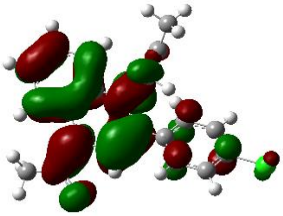
B: LUMO 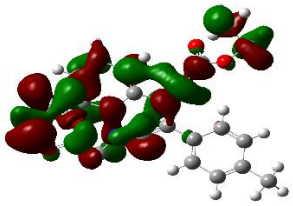	**B**: LUMO 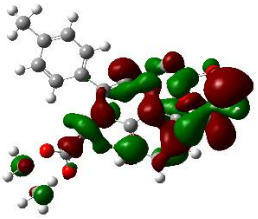
C: HOMO 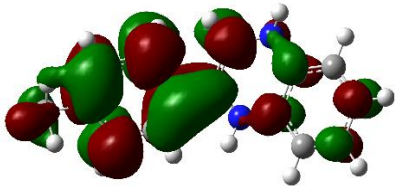	**C**: HOMO 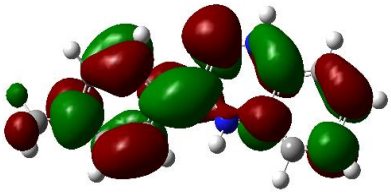
C: LUMO 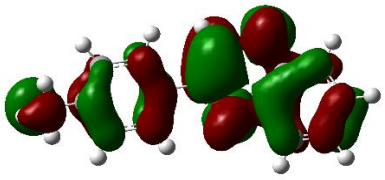	**C**: LUMO 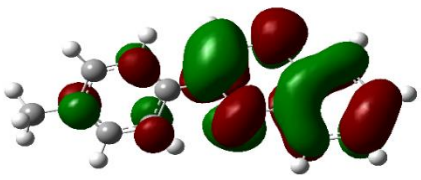

Fig. 3 – HOMO and LUMO of three inhibitors in the gas and aqueous phases.

Energy gap is an essential descriptor as a coefficient of the interaction of the inhibitor molecule against adsorption on the metal surface.[33] The reactivity of the molecule increases when the energy gap of the inhibitor is reduced. Corrosion inhibitors with small energy gaps are known to be effective. Because the ionization energy needed to remove the electron from the final occupied orbital is negligible.[34,35] Organic compounds are not only give electrons to empty metal orbitals, but also accept free electrons from the metal are usually good corrosion inhibitors.[36] Furthermore, a molecule with a small energy gap is more polarizable and usually associated with low kinetic stability and strong chemical activity, referred to as the soft molecule.[37] Table 1 demonstrates that inhibitor B has the lowest energy gap in all circumstances, indicating that the molecule might function better as a corrosion inhibitor. The following is the theoretical order for the fluctuation of inhibition efficiency of the examined inhibitors which fits with the actual data: B > A > C. Figure 3 shows LUMOs and HOMOs of selected molecules at B3LYP/6-311++G (d, p) basis set for non-protonated species in gas and aqueous phases.

Absolute hardness and softness are well-known qualities for determining molecule stability and reactivity. Chemical hardness is the resistance to displacement or polarization of the electron cloud, molecules, ions and atoms under minor perturbations of chemical reactions. A soft molecule has a tiny energy gap, whereas a hard molecule has a big energy gap.[38] As a result, molecules having the lowest global hardness values are projected to be effective corrosion inhibitors for bulk materials in acidic environments.[39] Adsorption of inhibitor onto a surface of the metal takes place in the softest and least hardened portion of the molecule. When it comes to molecular stability and reactivity, absolute hardness is a critical factor.[40] Soft molecules have higher reactivity than hard molecules since they can easily give electrons. As a result, inhibitors with the lowest global hardness values are projected to be effective corrosion inhibitors for bulk materials in acidic environments. Adsorption of inhibitor onto a metallic surface happens in the region of the molecule with the highest softness and lowest hardness.[41] Table 1 also show the computed values of the selected molecule as inhibitors in both aqueous and gas phases in comparison to protonated and non-protonated species. The computed values of the examined molecules in the gas and aqueous phases for non-protonated and protonated species are shown in Table 1. In comparison to inhibitor 2, the calculations show that inhibitors 1 and 2 have the greatest hardness levels. In comparison to quinoline derivatives, the B3LYP/6-311++G (d, p) data demonstrate that the hardness trend in the protonated aqueous phase is C, with a high hardness value of 2.43 eV. At the B3LYP/6-311++G (d, p) level of theory, a similar tendency is seen. The inhibitor with the lowest worldwide hardness value (and hence the highest global softness value) is likely to have the best inhibitory effectiveness. The following corrosion inhibition efficiency rating may be predicted based on our research: B > A > C. For the simplest electron transport, the results show that C and B have the highest hardness values.

The electronegativity of an atom in a molecule describes its tendency to draw electrons toward it.[42,43] Because excellent inhibitors are typically capable of donating electrons to the metallic surface, we predicted that as inhibitive efficiency improved, the electronegativity values would fall. In addition, Table 1 summarizes the values of the current system. The trend in the electronegativity values for the stated inhibitors demonstrates that B has the lowest value. When compared to A and C, this action boosts its adsorption on the mild steel surface and hence improves its corrosion prevention performance.

Polarizability (μ) refers to a molecule's capacity to be polarized, and it's a useful reactivity indicator. Increased polarizability values aid in the strong adsorption of corrosion inhibitors across metal surfaces, resulting in higher inhibition efficacy.[44] The ratio of the induced dipole moment to the electric field strength is known as polarizability. Polarizability is proportional to the generated dipole moment. The relationship between corrosion inhibitor polarizability and inhibition effectiveness has been a source of debate. Figure 4 illustrates the electrostatic potential map of selected molecule inhibitors in gas and aqueous phases.

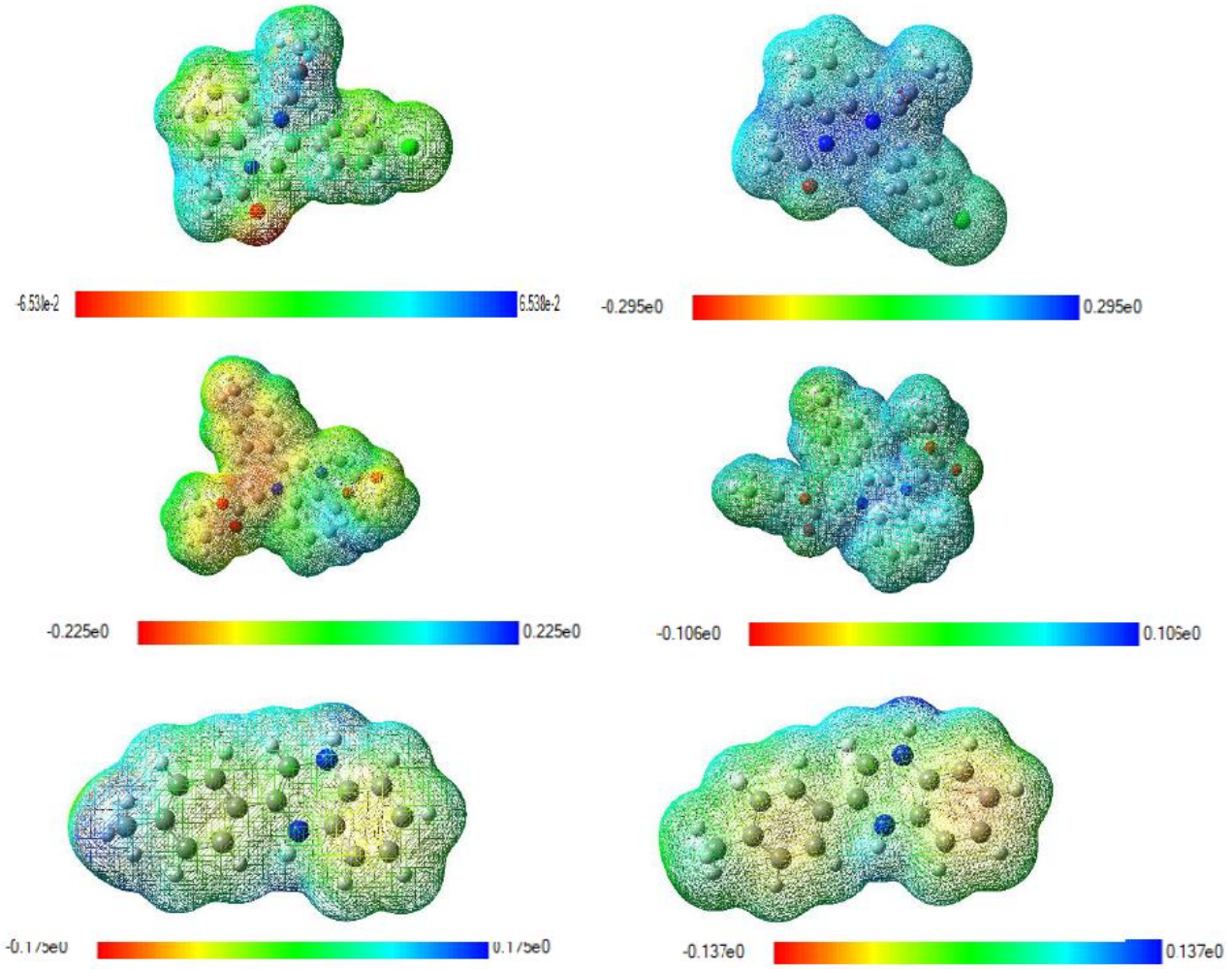

Gas phase Aqueous phase

Fig. 4 – Electrostatic potential map of the selected molecule inhibitors in gas and aqueous phase.

The minimum polarization principle (MPP) states that the normal course of evolution for each system is towards a less polarizable state.[45] The polarization of the three inhibitors was calculated in Table 1. As can be seen that the fluctuations in polarization follow the following pattern: B > A > C for non-protonated and protonated species, respectively. These results show that the pattern of increasing inhibitory inhibition efficiencies with respect to polarization improvement is similar to the results of experimental inhibition efficiencies by percentage (B > A > C).

Quantum chemical techniques compute total energy which is a useful metric. kinetic energy, internal and potential combine to make a system's total energy. In the appearance of a static external potential (for instance, the atomic nuclei), Hohenberg and Kohn established that the total energy of a system, including that of the many-body influences of electrons (exchange and correlation) is a unique function of the charge density.[46] The system's ground state energy is the minimal value of the total energy functional. The actual single-particle ground state energy is the electronic charge density that gives this minimum. The total energy of the best inhibitor B in our investigation is –1591.799, –1592.287, –1592.541 and –1532.232 (a.u) which is lower than the total energy of the compounds A and C.

Electrophilicity is a measure that assesses the willingness of a chemical species to take electrons. The highest value of electrophilicity has the greatest ability of the molecule to receive electrons. Thus, a good electrophile has high electrophile and chemical potential values, while a good nucleophile has a low electrophile and chemical potential. The compounds have low electrophilic index values which are excellent nucleophiles, but the lowest

value of electrophilicity has the highest capacity of the molecule to donate electrons as shown in Table 1. The electrophilic and nucleophilic values Table 1 can be used to rank the corrosion inhibition efficacy of the investigated compounds and have a good agreement with experimental results B > A > C.

Until the electronegativity and chemical potential equalize the electron moves from the lower to higher electronegativity when inhibitor and iron come closer to each other. Table 1 show the outcomes.[47] The positive number of electrons transmitted (ΔN) can be shown that the molecules are electron acceptors, whereas the negative number of electrons transferred (ΔN) can be shown that the molecules are electron donors. As a result, as the electron-donating capacity of these inhibitors to the metal surface rises, the inhibition efficiency increases. The inhibitory effectiveness rose with increasing electron-donating ability at the metal surface.[48] The quinolines investigated in this work have charge transfer properties towards mild steel. The value of ΔN_{max}< 3.6 eV denotes a molecule's proclivity to donate electrons to a metal surface. Table 1 can be also shown that the compounds under investigation are electron acceptors. The results have been shown that the largest proportion of electrons transported (ΔN_{max}) is linked to the best inhibitor (B), while the lowest fraction is linked to the inhibitor with the lowest inhibition efficacy (C). In all circumstances, the inhibitor molecules' capacity to accept electrons is in the sequence B > A > C. These findings are consistent with those of the experimental research.

An electronic back-donation mechanism may also control the interaction between the metal surface and the inhibitor molecule based on the charge transfer model for back-donation of charges.[49] According to this theory, if both electron transfer to the molecule and back-donation from the molecule occurs at the same time, the energy change is proportional to the molecule's hardness.[50] The following expression can calculate the back-donation energy[5,51]

$$\Delta E_{back-donation} = -\frac{\eta}{4} \qquad (8)$$

Back-donation from the molecule to the metal is energetically preferred when $\eta > 0$ or $\Delta E_{b-d} < 0$. Table 1 show that $\Delta E_{back-donation} = 0$, indicating that charge transfer to a molecule followed by back-donation from the molecule is dynamically advantageous.[9] If it is considered that the inhibition efficiency improves as the molecule adsorbs better to the metal surface, then the inhibition efficiency should increase as the stabilization energy generated by the interaction between the inhibitor rises and metal surface. The estimated ΔE_{b-d} values show the following tendency, as predicted and in agreement with the experimental data: B > A > C.

The initial molecule–metal interaction energy ($\Delta\psi$) determined by Sastri and Perumareddi which is another essential feature[52]

$$\Delta\psi = -\frac{(\chi_{Fe} - \chi_{inh})^2}{4(\eta_{Fe} + \eta_{inh})} \qquad (9)$$

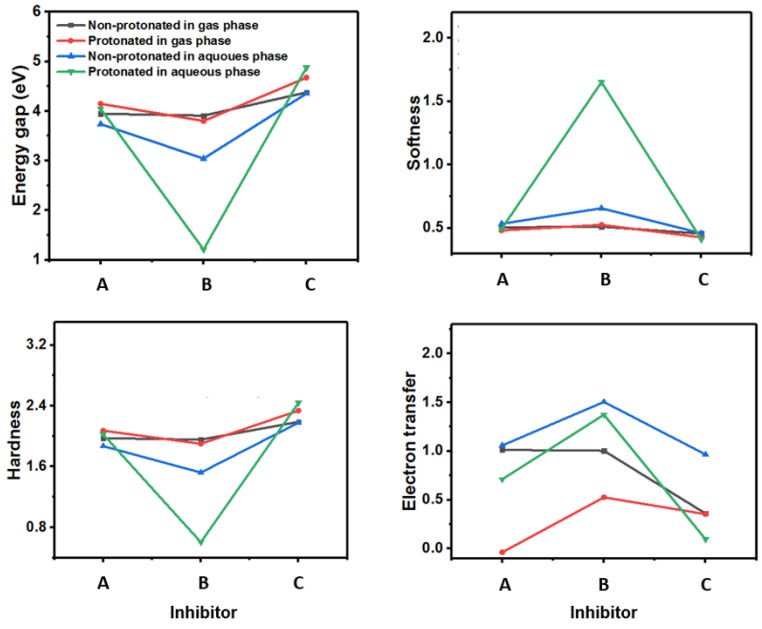

Fig. 5 – Global reactivity parameters of selected molecules.

The trend in molecule–metal interaction strength $|\Delta\psi|$ is also B > A, C based on the results of Table 1. In addition, B has the highest initial molecule–metal interaction energy ($\Delta\psi$), followed by B and A, while C has the lowest. Figure 5 shows global reactivity parameters of selected molecules for protonated and non-protonated species in gas and aqueous phases.

Monte Carlo computation

Monte Carlo simulations were run on a system comprised of inhibitor molecules and iron surface.[53,54] A Monte Carlo simulation using simulated annealing was performed after optimizing inhibitor compounds. Figure 6 shows the optimization energy curves for the inhibitor molecules before their placement on the iron surface.

Table 2 shows the outputs and descriptions. This contained the total energy of the substrate-adsorbate arrangement in kcal mol^{-1}. Total energy is defined as the sum of adsorbate component energies, deformation energy and rigid adsorption energy. Adsorption energy is the amount of energy generated (or required) when the relaxed adsorbate components are adsorbed on the substrate in this investigation. Table 2 also includes (dE_{ads}/dN_i) which indicates the energy in kcal mol^{-1}, of substrate–adsorbate combinations with one of the adsorbate components removed. All of the inhibitors have negative adsorption energy. This shows that they can adsorb on the iron Fe (110) surfaces.

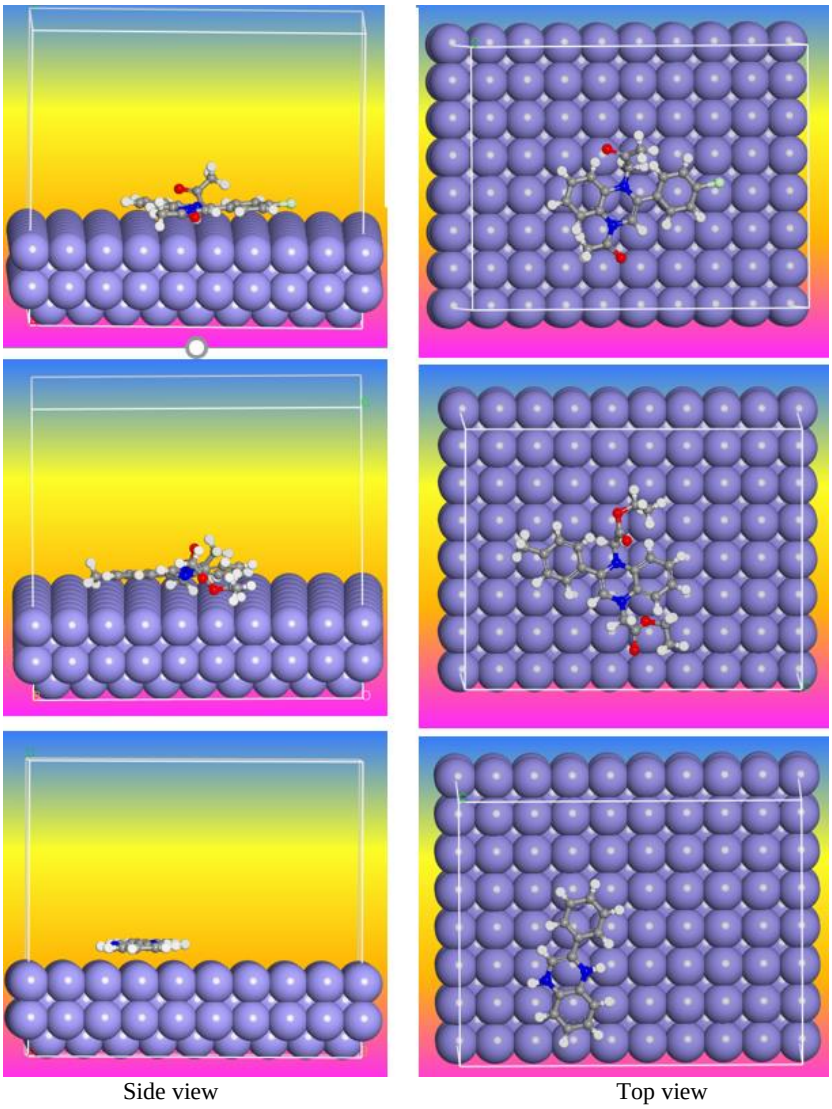

Side view Top view

Fig. 6 – Molecular simulations for the most favorable modes of adsorption obtained for the selected molecules on Fe (110) surface.

Table 2

The outputs and descriptors calculated by the Monte Carlo simulation for adsorption of selected inhibitors on Fe (110) (in kcal mol^{-1}) and experimental inhibition efficiency

Inhibitor	Total energy	Adsorption energy	Rigid adsorption	Deformation energy	$\frac{dE_{ad}}{dN_i}$	Experimental efficiency %
A	1.136169×10^4	–146.59327844	–146.59327841	–3.211426e-008	–146.59327844	95.8
B	278.91817500	–160.46101002	–160.46101002	–1.108447e-011	–160.46101002	97
C	79.10273761	–103.05468466	–103.05468466	–1.770957e-010	–103.05468466	86.1

The effect concentration on corrosion

Three other studies were used to prove that our results are valid, and these studies were practical studies. To determine the activation energy and investigate the uniform mechanism of the corrosion process, temperature conversion for weight loss is the significant mechanism. In this part, the effect of temperature and focus on corrosion inhibition efficiency explained.[2] It is self-evident that as the temperature increased, corrosion rates increased as well. This increase in corrosion rate with temperature is due to the increase in the conductivity of ionic species, resulting in thermal mixing of ions, thus leading to an increase in conductivity. In those other phrases, the counter ions (NO_3^-) and transfer of the acid's aggressive ions (H^+) affect the rate of corrosion. Each inhibitor's main function is to adsorb on the metal surface, producing a barrier even against the entrance of H^+. The type and concentration of the inhibitor, as well as the temperature and stirring influence the interaction between the metal surface and the inhibitor. The effect of temperature on the corrosion behavior of steel/acid in the absence and presence of inhibitors in this study at various concentrations is explored using a weight-loss trend at temperatures ranging from 308 to 343°K. At low concentrations, the rise is more affected. The findings also show that when the inhibitor concentration increased, the corrosion rate of carbon steel reduced at a given temperature. As the inhibitor concentration is increased, the effectiveness of inhibition expands. Figure 7 can be shown that the optimal concentration necessary to achieve efficiency was discovered. The inhibition by inhibitors can be described in terms of metal surface adsorption. The interaction between the metal surface allows the molecule to be adsorbed and the lone pair of electrons on the nitrogen atom of the quinoxaline. The existence of low-energy empty orbitals in the iron atom facilitates this reaction, as seen in transition group metals. Furthermore, in acidic solutions, the production of positively charged protonated inhibitors A, B and C species enhances the adsorption of the compound on the metal surface via electrostatic interactions between the metal surface and the organic molecules.

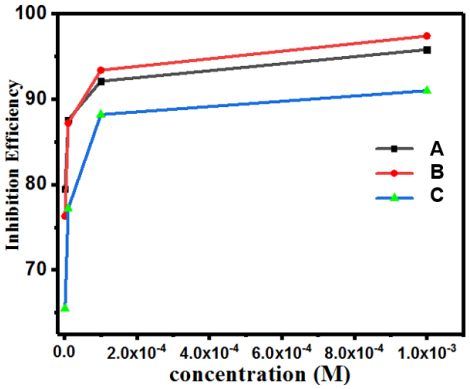

Fig. 7 – Variation of inhibition efficiency with the concentration of A, B and C.

The effect of temperature on corrosion inhibition efficiency

Corrosion is caused by an electrochemical reaction between the cathodic and anodic areas of an alloy or metal which are connected by a metallic and electrical channel. For example, a pipe or structure connected to water in offshore installations. Frequency and degree of corrosion are influenced by the temperature, pressure, composition of the surrounding fluid, and physical characteristics of the flow. These variables affect corrosion and, consequently, corrosion model predictions. The rate of electrochemical corrosion of metal is greatly affected by temperature. Increases in temperature favor the overcapacity of oxygen transport and depolarization of oxygen in neutral solution (oxygen depolarization), but decrease oxygen solubility. Since hydrogen evolution decreases with increasing temperature in an acidic medium, the corrosion rate grows exponentially with increasing temperature. An

Arrhenius plot equation can be used to evaluate the effect of temperature and activation factors on different systems.

Several studies have been conducted on the corrosion of molecules in acidic environments. They discovered that the corrosion percentage increased with increasing temperature in inhibited solutions, but the inhibition efficacy decreased with increasing temperature. Poor physical adsorption may be the reason for the lower inhibition efficiency when the temperature is raised in the presence of the inhibitor. Figure 8 shows the effect of temperature of investigated inhibitors on corrosion inhibition efficiency.

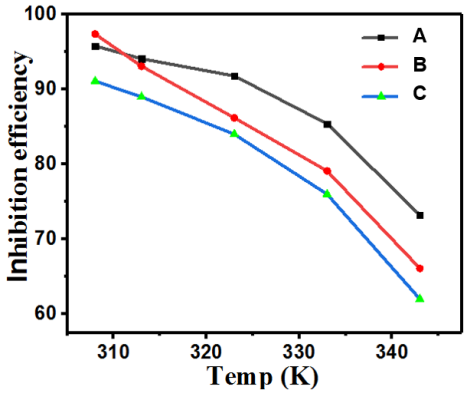

Fig. 8 – The effect of temperature of investigated inhibitors.

CONCLUSIONS

DFT calculations and acquired data are used to investigate the inhibitory effectiveness of various quinoxalines. The inhibitory efficacy of three substituted quinoxaline molecules can be linked to their molecular structure using B3LYP level at 6-311++G (d, p) basis set. It is estimated that computed dipole moments have a high correlation with corrosion inhibition efficiency and they are also associated with other quantum chemical parameters such as softness, energy gap and hardness. Monte Carlo calculations indicate that higher negative adsorption energies of investigated inhibitors demonstrate more stable and stronger interactions between Fe (110) and inhibitor molecules. The negative values of adsorption energies of quinoline molecules on the Fe (110) surface increase in the order B > A > C. This is consistent with the experimental findings, indicating that chemical B has the highest inhibitory effectiveness. The inhibition efficiency of the inhibitors has an opposite relationship with temperature, at a lower temperature indicates higher efficiency, but at a higher concentration, the inhibition efficiency increases. In this study, there was no contradiction between simulation and practice to determine the corrosion level of materials. This is very good evidence to rely on simulation calculations.

REFERENCES

1. M. Chigondo and F. Chigondo, *J. Chem.*, **2016**, *2016*, 1–7.
2. A. Lesar and I. Milošev, *Chem. Phys. Lett.*, **2009**, *483*, 198–203.
3. A. Zarrouk, B. Hammouti, A. Dafali, M. Bouachrine, H. Zarrok, S. Boukhris and S.S. Al-Deyab, *J. Saudi Chem. Soc.*, **2014**, *18*, 450–455.
4. A. Zarrouk, B. Hammouti, S. Al-Deyab, R. Salghi, H. Zarrok, C. Jama and F. Bentiss, *Int. J. Electrochem. Sci.*, **2012**, *7*, 5997–6011.
5. D.M. Mamand, H.H. Rasul, P.K. Omer and H.M. Qadr, *Condensed Matter and Interphases*, **2022**, *24*, 227–242.
6. H.M. Qadr, *Phys. Part. Nucl.*, **2021**, *18*, 185–189.
7. H.M. Qadr, *Russ. J. Non-Ferr.*, **2021**, *62*, 561–567.
8. G. Gece and S. Bilgiç, *Corr. Sci.*, **2009**, *51*, 1876–1878.
9. H.M. Qadr and D.M. Mamand, *J. Bio- Tribo-Corros.*, **2021**, *7*, 1–8.
10. L. Guo, X. Ren, Y. Zhou, S. Xu, Y. Gong and S. Zhang, *Arab. J. Chem.*, **2017**, *10*, 121–130.
11. M. Dehdab, M. Shahraki and S.M. Habibi-Khorassani, *Amino acids*, **2016**, *48*, 291–306.
12. A. Zarrouk, M. Messali, M. Aouad, M. Assouag, H. Zarrok, R. Salghi, B. Hammouti and A. Chetouani, *J. Chem. Pharm. Res.*, **2012**, *4*, 3427–3436.
13. H.M. Qadr, *Gazi Univ. J. Sci.*, **2022**, *35*, 272–279.
14. L.M. Rodríguez-Valdez, A. Martínez-Villafañe and D. Glossman-Mitnik, *J. Molec. Struct.: Theochem*, **2005**, *713*, 65–70.
15. M.K. Awad, M.R. Mustafa and M.M.A. Elnga, *J. Molec. Struct.: Theochem.*, **2010**, *959*, 66–74.
16. H.M. Qadr, *At. Indones.*, **2020**, *46*, 47–51.
17. P. Geerlings and F. De Proft, *Int. J. Molec. Sci.*, **2002**, *3*, 276–309.
18. H. Zarrok, A. Zarrouk, R. Salghi, H. Oudda, B. Hammouti, M. Assouag, M. Taleb, M. Ebn Touhami, M. Bouachrine and S. Boukhris, *J. Chem. Pharm. Res.*, **2012**, *4*, 5056–5066.
19. H. Zarrok, A. Zarrouk, R. Salghi, M. Assouag, B. Hammouti, H. Oudda, S. Boukhris, S.Al Deyab and I. Warad, *Der Pharmacia Lettre*, **2013**, *5*, 43–53.
20. H. Zarrok, A. Zarrouk, R. Salghi, H. Oudda, B. Hammouti, M.E. Touhami, M. Bouachrinee and S. Boukhris, *Portugaliae Electrochimica Acta*, **2012**, *30*, 405–417.
21. M.M. Kabanda, I.B. Obot and E.E. Ebenso, *Int. J. Electrochem. Sci.*, **2013**, *8*,
22. R. Silaghi-Dumitrescu and I. Silaghi-Dumitrescu, *Rev. Roum. Chim.*, **2004**, *49*, 257–268.
23. D.M. Mamand, T.M.K. Anwer and H.M. Qadr, *Oxid. Commun.*, **2022**, *45*, 600–627.
24. L. Hu, X. Huang, Q. Zeng, Y. Wang and S. Li, *Rev. Roum. Chim.*, **2022**, *67*, 321–328.
25. I. Obot and Z. Gasem, *Corr. Sci.*, **2014**, *83*, 359–366.
26. N.A. Wazzan, O.S. Al-Qurashi and H.M. Faidallah, *J. Molec. Liquids*, **2016**, *223*, 29–47.

27. H. Elmsellem, T. Harit, A. Aouniti, F. Malek, A. Riahi, A. Chetouani and B. Hammouti, *Prot. Met. Phys. Chem. Surf.*, **2015**, *51*, 873–884.
28. S. Kaya, B. Tüzün, C. Kaya and I.B. Obot, *J. Taiwan Institute of Chemical Engineers*, **2016**, *58*, 528–535.
29. E. Honarmand, H. Mostaanzadeh, M.H. Motaghedifard, M. Hadi and M. Khayadkashani, *Prot. Met. Phys. Chem. Surf.*, **2017**, *53*, 560–572.
30. N. Khalil, *Electrochimica Acta*, **2003**, *48*, 2635–2640.
31. H.M. Qadr and D.M. Mamand, *Azerbaijan Chem. J.*, **2023**, 19–29.
32. D.M. Mamand and H.M. Qadr, *Himia, Fizika ta Tehnologia Poverhni*, **2023**, *14*, 159–172.
33. D.M. Mamand and H.M. Qadr, *Protect. Met. Phys. Chem. Surface.*, **2021**, *57*, 943–953.
34. E.E. Ebenso, T. Arslan, F. Kandemirli, N. Caner and I. Love, *Int. J. Quantum Chem.*, **2010**, *110*, 1003–1018.
35. G. Bereket, E. Hür and C. Öğretir, *J. Molec. Struct.: Theochem.*, **2002**, *578*, 79–88.
36. I. Obot, S. Kaya, C. Kaya and B. Tüzün, *Physica E: Low-dimensional Systems and Nanostructures*, **2016**, *80*, 82–90.
37. V. Choudhary, A. Bhatt, D. Dash and N. Sharma, *J. Comput. Chem.*, **2019**, *40*, 2354–2363.
38. M. Shahraki, M. Dehdab and S. Elmi, *J. Taiwan Institute of Chem. Engineers*, **2016**, *62*, 313–321.
39. B. Rani and B.B.J. Basu, *Int. J. Corr.*, **2012**, *2012*,
40. I. Obot and N. Obi-Egbedi, *Corr. Sci.*, **2010**, *52*, 198–204.
41. D.M. Mamand and H.M. Qadr, *Russ. J. Phys. Chem. A.*, **2022**, *96*, 2155–2165.
42. P. Singh, V. Srivastava and M. Quraishi, *J. Molec. Liquids*, **2016**, *216*, 164–173.
43. S. Kaya, C. Kaya and N. Islam, *Computational and Theoretical Chemistry*, **2016**, *1080*, 72–78.
44. H. Lgaz, R. Salghi, S. Masroor, S.-H. Kim, C. Kwon, S.Y. Kim, Y.-J. Yang and I.-M. Chung, *J. Molec. Liquids*, **2020**, *308*, 112998.
45. S. Esmailzadeh, M. Aliofkhazraei and H. Sarlak, *Prot. Met. Phys. Chem. Surf.*, **2018**, *54*, 976–989.
46. H. Ju, Z.-P. Kai and Y. Li, *Corr. Sci.*, **2008**, *50*, 865–871.
47. S. Martinez, *Mater. Chem. Phys.*, **2003**, *77*, 97–102.
48. I. Lukovits, E. Kalman and F. Zucchi, *Corrosion*, **2001**, *57*, 3–8.
49. B. Gómez, N.V. Likhanova, M.A. Domínguez-Aguilar, R. Martínez-Palou, A. Vela and J.L. Gazquez, *J. Phy. Chem., B*, **2006**, *110*, 8928–8934.
50. D.M. Mamand, A.H. Awla, T.M.K. Anwer and H.M. Qadr, *Chim. Techno Acta*, **2022**, *9*, 20229203.
51. D.M. Mamand, T.M. Anwer, H.M. Qadr and C.H. Mussa, *Russ. J. Gen. Chem.*, **2022**, *92*, 1827–1838.
52. V. Sastri and J. Perumareddi, *Corrosion*, **1997**, *53*.
53. L. Guo, S. Zhu and S. Zhang, *J. Ind. Engineer. Chem.*, **2015**, *24*, 174–180.
54. Ş. Erdoğan, Z.S. Safi, S. Kaya, D.Ö. Işın, L. Guo and C. Kaya, *J. Molec. Structure*, **2017**, *1134*, 751–761.